Chaotic dynamics of a nonlinear density dependent population model

View the article online for updates and enhancements.

Chaotic dynamics of a nonlinear density dependent population model

Ilie Ugarcovici and Howard Weiss

Department of Mathematics, The Pennsylvania State University, University Park, PA 16802, USA

E-mail: idu@math.psu.edu and weiss@math.psu.edu

Abstract
We study the dynamics of an overcompensatory Leslie population model where
the fertility rates decay exponentially with population size. We find a plethora
of complicated dynamical behaviour, some of which has not been previously
observed in population models and which may give rise to new paradigms in
population biology and demography.

   We study the two- and three-dimensional models and find a large variety of
complicated behaviour: all codimension 1 local bifurcations, period doubling
cascades, attracting closed curves that bifurcate into strange attractors, multiple
coexisting strange attractors with large basins (which cause an intrinsic lack of
'ergodicity'), crises that can cause a discontinuous large population swing,
merging of attractors, phase locking and transient chaos. We find (and explain)
two different bifurcation cascades transforming an attracting invariant closed
curve into a strange attractor. We also find one-parameter families that exhibit
most of these phenomena. We show that some of the more exotic phenomena
arise from homoclinic tangencies.

Mathematics Subject Classification: 37D45, 37G35, 37N25, 92D25

(Some figures in this article are in colour only in the electronic version)

1. Introduction

Population biologists and ecologists need accurate population models to predict animal
population sizes and compositions. Models help with wildlife management and establishing
harvesting limits and could be of tremendous help in conservation efforts. Governments and
businesses need reliable age-structured demographic models to project Social Security outlays,
Medicare outlays, education outlays, tax receipts, set immigration policy, etc.

Virtually all animal population and demographic forecasting models in current use are based on variations of the age-structured linear Leslie model (see section 2). Perhaps not coincidentally, the 2000 US census 'shocked demographers': it showed that the best demographic models based on 1990 census data underestimated the US population by six million people [37]. Many population biologists and demographers now look to nonlinear models for more accurate population models and projections.

In this paper, we study the dynamics of the overcompensatory Leslie population model where the fertility rates decay exponentially with population size [4,7,11,18,28,31,32,34,36]. Caswell highlights this nonlinear and noninvertible model in the introduction of the second edition of his influential treatise [4], as well as in a latter section, and we think it fair to infer that he is championing this nonlinear model as a prototype for the next generation of population models. This investigation is the first step of our programme to study systematically the global dynamics and bifurcations for nonlinear Leslie models where the fertility rates and survival probabilities have various natural functional forms as functions of the population size including exponential decay, inverse polynomial decay, unimodal dependence and bimodal dependence. Our ultimate goal is to create a 'population modelling toolbox' that could be used by a wide range of population modellers to predict animal populations more accurately.

In the two- and three-generation versions of this overcompensatory model, through careful numerical studies, we find a plethora of complicated dynamical behaviour: several codimension 1 local bifurcations, period doubling cascades, attracting closed curves that bifurcate into strange attractors, three routes to chaos, multiple coexisting strange attractors with large basins (which cause an intrinsic lack of 'ergodicity'), crises (interior, boundary—which can cause a discontinuous large population swing), merging of attractors, phase locking, transient chaos, and nonuniform hyperbolicity. We also find one-parameter families that exhibit most of these phenomena. We show that some of the more exotic phenomena arise from homoclinic tangencies. We cannot help stress that the variety of complicated dynamical phenomena in these one-parameter families of smooth maps of $\mathbb{R}^2$ and $\mathbb{R}^3$ is bewildering and is much more complicated than any other nonlinear population model in the literature that we have checked.

Many of these phenomena have not been previously observed in population models and may give rise to new paradigms in population biology and demography. For instance, this overcompensatory Leslie model exhibits crises (collisions of (strange) attractors with unstable periodic orbits), which can result in very large and discontinuous population changes. Grebogi *et al* initiated a comprehensive study of these phenomena (see [10]). Crises might help explain some seemingly 'bizarre' population explosions or collapses, like the current sardine explosion off the waters of northern California [5]. We stress that the existence of crises 'causing' large and discontinuous population swings result from a special type of chaotic behaviour of the system, and this is a striking consequence to populations of chaos.

We find and explain two different complicated bifurcation cascades transforming an attracting invariant closed curve 'into' a strange attractor—a seemingly new path to chaos in population models. The cascade in the two-dimensional model begins with phase locking and the destruction of an invariant curve, while the cascade in the three-dimensional case begins with a Hopf bifurcation. Period doubling cascades and crises play an essential role in both cascades. While one can find several models in the dynamics literature where an invariant closed curve seems to bifurcate into a strange attractor [1, 6, 9, 35], these are the first two examples for population models, and we have a complete understanding of the complicated sequence of intermediate (local and global) bifurcations.

Population biologists call a model (or the population it describes) *ergodic* if the asymptotic dynamics are independent of the initial conditions. To them, ergodic models are useful

because population patterns might reveal something about the underlying process rather than initial conditions. Most population biologists seem to strongly believe that what is important is the underlying population process and the initial conditions are historical accidents, and thus ergodicity is a fundamental element in models. We discovered parameter ranges with coexisting strange attractors with large basins in which this notion of ergodicity fails in an essential way. This may help change population biologists' views of the roles of ergodicity and initial conditions. We are currently studying the existence and statistical properties of SRB, or natural measures on these attractors, which should also help make the notion of ergodicity more rigorous.

We remark that for this nonlinear model most of the complicated dynamics only occur for large fertility rates (fish, small mammals, insects, etc). Although we are currently unaware of any animal whose population can be accurately forecast using this precise model, this model exhibits many complicated dynamical phenomena and paradigms that seem likely to arise in the next generation of population models.

In a landmark work, Cushing and co-workers [8] modelled the population growth of laboratory populations of flour beetles. They derived a nonlinear model starting from the three-generation Leslie model and incorporated the effect of cannibalism caused by overpopulation stress. They show that for certain parameter ranges the system has a strange attractor. Remarkably, they observe this chaotic behaviour in the laboratory. This work has been hailed as the first verifiable example of chaos in ecology. We also refer the reader to [8] for an enlightening discussion of the difficulties of biological modelling. We remark that this beetle model exhibits a much smaller variety of complicated dynamical behaviour than does the model we study in this paper.

Finally, we outline the structure of this paper. In section 2, we briefly describe the (linear) Leslie model. In section 3, we introduce the nonlinear extension of this model and in section 4 some of the basic properties are described. In section 5, we analyse the dynamics for the two-generation version of the model. Most of the complicated dynamical phenomena we observe for the three-generation model already appear in a one-parameter family for the two-generation model. We have not found any dynamical phenomenon that does not occur in at least one of the two special parametrized families we analyse. In section 6, we discuss the differences between two- and three-generation models. In the appendix, we briefly review some useful concepts from dynamical systems, including the definition of stable and unstable manifolds, dominant Lyapunov exponents, strange attractors, Hénon-like attractors and crises.

2. The linear Leslie model

About 60 years ago, Leslie introduced the following age-structured linear population model [16, 17]. Consider a population divided into d age-classes or generations, which we call generations $1, 2, \ldots, d$. Let $n_k(t)$ be the number of individuals in the kth age-class at time t, measured in generations. The individuals in generations $2, \ldots, d$ are survivors of the previous generation at time t, and thus one assumes that for $2, 3, \ldots, d$

$$n_k(t + 1) = p_{k-1} n_{k-1}(t),$$

where $p_i, i = 1, \ldots, p_{d-1}$ is the probability that an individual of age-class i survives for one generation. The new members of age-class 1 cannot be survivors of any other age-class; they must have originated from reproduction. Thus, Leslie assumed

$$n_1(t + 1) = f_1 n_1(t) + f_2 n_2(t) + \cdots + f_d n_d(t),$$

where f_i is the *per capita* fertility of generation i. Hence

$$\begin{pmatrix} n_1 \\ n_2 \\ \vdots \\ n_d \end{pmatrix}(t+1) = \begin{pmatrix} f_1 & f_2 & \cdots & f_{d-1} & f_d \\ p_1 & 0 & \cdots & 0 & 0 \\ \vdots & \vdots & \cdots & \vdots & \vdots \\ 0 & 0 & \cdots & p_{d-1} & 0 \end{pmatrix} \begin{pmatrix} n_1 \\ n_2 \\ \vdots \\ n_d \end{pmatrix}(t),$$

or more compactly,

$$\mathbf{n}(t+1) = A\mathbf{n}(t).$$

This special age-classified matrix A is called the *Leslie matrix*. The matrix A is non-negative with positive entries only in the first row and the subdiagonal. Population biologists and demographers use life table analysis to construct the matrix A.

Since A has non-negative entries and A^d has positive entries (for quite general conditions on $f_1, f_2, \ldots, f_d$), the Perron–Frobenius theorem gives the stable age distribution. More precisely, if λ_1 is the spectral radius of A, then

$$\lim_{t \to \infty} \left(\frac{1}{\lambda_1} A \right)^t = \mathbf{v} \otimes \mathbf{w}^T,$$

where $\mathbf{v}$ and $\mathbf{w}$ are normalized left and right eigenvectors for λ_1.

Most Leslie models used for actual demographic forecasting use 5-year age groups instead of three generations, in which case the matrix A becomes a 10×10 matrix. The text 'Matrix Population Models' by Caswell [4] contains a comprehensive treatment of Leslie models.

3. The nonlinear Leslie model

We now consider the Leslie population model where the fertility rates decay exponentially with population size (Ricker-type nonlinearity). In this case, the Leslie matrix A becomes the population-size dependent matrix

$$A(N) = \begin{pmatrix} f_1 e^{-\lambda N} & f_2 e^{-\lambda N} & \cdots & f_{d-1} e^{-\lambda N} & f_d e^{-\lambda N} \\ p_1 & 0 & \cdots & 0 & 0 \\ \vdots & \vdots & \cdots & \vdots & \vdots \\ 0 & 0 & \cdots & p_{d-1} & 0 \end{pmatrix}.$$

One obtains the following system of d *nonlinear* equations

$$n_1(t+1) = (f_1 n_1(t) + f_2 n_2(t) + \cdots + f_d n_d(t)) e^{-\lambda(n_1(t)+n_2(t)+\cdots+n_d(t))}$$
$$n_2(t+1) = p_1 n_1(t)$$
$$\vdots$$
$$n_d(t+1) = p_{d-1} n_{d-1}(t).$$

The associated $2d$-parameter nonlinear dynamical system $T : \mathbb{R}^d \to \mathbb{R}^d$ is

$$T \begin{pmatrix} x_1 \\ x_2 \\ \vdots \\ x_d \end{pmatrix} = \begin{pmatrix} (f_1 x_1 + f_2 x_2 + \cdots + f_d x_d) \cdot e^{-\lambda(x_1+x_2+\cdots+x_d)} \\ p_1 x_1 \\ \vdots \\ p_{d-1} x_{d-1} \end{pmatrix}. \tag{1}$$

Note that when $\lambda = 0$ this model reduces to the classical Leslie matrix model.

For two and three generations, the corresponding systems are

$$T(x, y) = ((f_1 x + f_2 y) \cdot e^{-\lambda(x+y)}, p_1 x) \tag{2}$$

and

$$T(x, y, z) = ((f_1 x + f_2 y + f_3 z) \cdot e^{-\lambda(x+y+z)}, p_1 x, p_2 y), \tag{3}$$

respectively.

In [11], the authors study a special case of (2) when $f_1 = f_2$ and $p_1 = 1$; they analyse the stability of the nontrivial fixed point, finding four types of codimension 1 local bifurcations: transcritical, saddle-node, Hopf and period doubling. Numerically, they also find a 'strange attractor' obtained after a period doubling cascade. However, they largely ignore the investigation of multiple stable states and crisis phenomena. Levin and Goodyear [18] effected a local analysis for a related fish population model. In their seminal paper [36], Wilkan and Mjølhus rigorously study the stability of the positive fixed point for two-, three- and four-generation models and study the codimension 1 local bifurcations. They find parameter values where a stable period-3 orbit coexists with an invariant closed curve, and they observe the destruction of the closed curve. They also find parameter values where there exists a three-piece strange attractor.

Some of the complicated dynamical phenomena we observe for the two-generation nonlinear Leslie model have also been observed for the famous Hénon mapping [13, 33], $H : \mathbb{R}^2 \to \mathbb{R}^2$, $H(x, y) = (a - by - x^2, x)$ where a and b are real parameters. The mapping H is a quadratic polynomial and is easily seen to be a diffeomorphism. The Jacobian determinant is the constant function b. Benedicks and Carleson [4] proved that for a positive measure set of parameter values with $1 \leqslant a \leqslant 2$ and $b \approx \exp(-20)$, the mapping H has a nonhyperbolic attractor with a dense orbit and has a positive Lyapunov exponent. For the parameter values they study, the Hénon mapping is a tiny perturbation of a one-dimensional quadratic mapping, and this is crucial for their analysis. Very little has been proven about this mapping for larger values of b; see [14, 21] for the existence of transversal homoclinic intersections and hence hyperbolic horseshoes.

For comparison, the overcompensatory Leslie model is not a polynomial mapping, it is not a diffeomorphism and it is not usually dissipative (the modulus of the Jacobian matrix does not have a determinant less than 1). Not surprisingly, we cannot prove very much about the global dynamics. We effect a careful numerical study and attempt a theoretical interpretation of our numerical study and numerical experiments. *A priori*, our strange attractors could be periodic orbits having a huge period (e.g. 10^7 generations). However, possibilities like this seem totally irrelevant to the application at hand.

Our goal for the remainder of this paper is to investigate the dynamics of the mapping T and the implications for the population.

4. General facts about the nonlinear Leslie model

Before we proceed with the detailed analysis of two- and three-generation models, we make some general observations about the mapping T. For ease of exposition, we will consider the three-generation case.

(1) The *nonlinear mapping T* is C^∞ smooth. It is *noninvertible*; every point has at most two preimages under T. *A priori*, noninvertibility greatly complicates the analysis of a dynamical system. Although the local stable and unstable manifolds exist and have the usual properties (see appendix), the global manifolds are not always well defined, and even if they are, they could have nasty pathologies like cusps and self-intersections. In the two-dimensional model,

for all the parameter values we have studied, the degeneracy locus (see (6) for a description) does not intersect any important dynamical objects (e.g. attractors, stable or unstable manifolds of key periodic orbits, etc), and thus the noninvertibilty seems to have a benign influence on the dynamics. As far as we can tell the same is true for the three-dimensional model, with the possible exception of the noninvertibility being responsible for the 'thickening' of the strange attractor (see section 6.1), which we do not yet understand.

(2) If $f_1 + f_2 p_1 + f_3 p_1 p_2 < 1$, the origin $(0, 0, 0)$ is a global attractor for T (see [7, 36] for details). The quantity $f_1 + f_2 p_1 + f_3 p_1 p_2$ is the average *per capita* number of offspring that each member produces over its lifetime, assuming $\lambda = 0$, or no overcompensation. The statement implies that if, without the overcompensation, the average number of offspring per individual per lifetime is less than one, then the population becomes extinct over time.

(3) T is *pointwise dissipative* [7, 12], i.e. there exists a trapping region R that absorbs *every* orbit after a finite number of iterations of T. Indeed, every orbit, after two iterations, gets mapped into the box

$$R = \{0 \leqslant x \leqslant r, \ 0 \leqslant y \leqslant p_1 r, \ 0 \leqslant z \leqslant p_1 p_2 r\},$$

where $r = (f_1 + f_2 + f_3)/(\lambda e)$. It follows that the set

$$\Lambda = \bigcap_{n=1}^{\infty} T^n(R)$$

is a global attractor. In general, this attractor is not transitive, but we will try to identify the transitive components.

(4) If $f_1 + f_2 p_1 + f_3 p_1 p_2 > 1$, the mapping T has a unique positive fixed point at $(a, p_1 a, p_1 p_2 a)$ where

$$a = \frac{1}{\lambda} \cdot \frac{\log(f_1 + f_2 p_1 + f_3 p_1 p_2)}{(1 + p_1 + p_1 p_2)}.$$

Moreover, the origin $(0, 0, 0)$ is unstable, and the dynamical system is *uniformly persistent* with respect to $(0, 0, 0)$, i.e. there exists $C > 0$ such that if $(x_0, y_0, z_0) \in \mathbb{R}_+^3 \backslash \{0, 0, 0\}$, then $\liminf_{n \to \infty} |x(n) + y(n) + z(n)| > C$ (see [7] for details).

(5) It is easy to compute the linearization of the map T. The Jacobian, $J_T(x, y, z)$, of T at (x, y, z) is

$$\begin{pmatrix} e^{-\lambda(x+y+z)}(f_1 - \lambda \bar{f}) & e^{-\lambda(x+y+z)}(f_2 - \lambda \bar{f}) & e^{-\lambda(x+y+z)}(f_3 - \lambda \bar{f}) \\ p_1 & 0 & 0 \\ 0 & p_2 & 0 \end{pmatrix},$$

where $\bar{f} = \bar{f}(x, y, z) = f_1 x + f_2 y + f_3 z$. The determinant of the Jacobian is

$$\det(J_T(x, y, z)) = e^{-\lambda(x+y+z)} p_1 p_2 (f_3 - \lambda(f_1 x + f_2 y + f_3 z)).$$

The mapping T is said to be *dissipative* if $|\det J_T| < 1$. In the special case $f = f_1 = f_2 = f_3$, the map is dissipative if

$$p_1 p_2 f |1 - \lambda(x + y + z)| < e^{\lambda(x+y+z)}.$$

Clearly, if $p_1 p_2 f < 1$, then T is dissipative.

(6) The mapping T is a local diffeomorphism at a point (x, y, z) if $\det J_T(x, y, z) \neq 0$. If $\det J_T(x, y, z) = 0$ we call this point degenerate. We define the *degeneracy locus*, $\mathcal{D}$, to consist of all the degenerate points. Thus $\mathcal{D}$ is the plane $f_1 x + f_2 y + f_3 z = f_3/\lambda$.

(7) The parameter λ is just a rescaling factor for the mapping T, and thus the dynamics does not depend on the particular choice of λ. In particular

$$T(\lambda; x, y, z) = \frac{1}{\lambda} T(1; \lambda x, \lambda y, \lambda z).$$

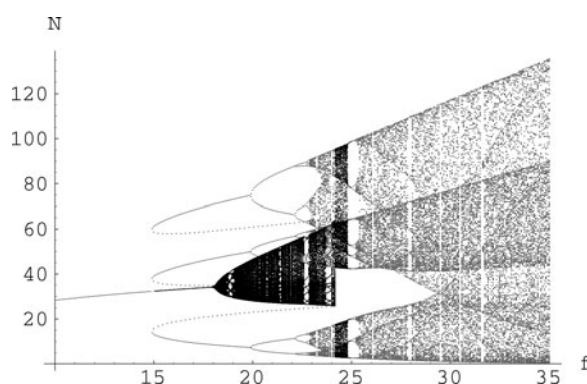In all our numerical simulations, $\lambda = 0.1$.

Figure 1. Bifurcation diagram: $10 \leqslant f \leqslant 35$.

5. The two-generation model

In this section, we study the two-generation model with equal fertility rates $f = f_1 = f_2$ and fixed survival probability $p_1 = 0.7$,

$$T(x, y) = (f \cdot (x + y)e^{-0.1(x+y)}, 0.7x).$$

We have chosen this value of p_1 to illustrate the complicated dynamics one obtains and, in particular, the existence of multiple strange attractors with large basins of attraction. This remarkable one-parameter family exhibits all the complicated dynamics we have so far observed for the two-generation model and also contains almost all the complicated dynamics we have so far observed for the three-generation model.

We briefly remark that for $0 < p_1 < \frac{1}{2}$ the dynamical system undergoes a period doubling route to chaos [36]. If $\frac{1}{2} < p_1 < 1$, then the fixed point undergoes a supercritical Hopf bifurcation at

$$f_H = \frac{1}{1 + p_1}e^{(1+2p_1)/p_1} \approx 18.13.$$

This type of bifurcation cannot occur for one-dimensional maps. Using the observations made in the previous section, we have, for $0 < f < 1/(1 + p_1) = 0.588$, the origin $(0, 0)$ is a global attractor. If $f > 0.588$, there exists a positive fixed point (equilibrium solution) that is asymptotically stable for small enough f. For $0.588 < f < 14.9$, the equilibrium solution is a global attractor.

Figure 1 shows the bifurcation diagram for $10 \leqslant f \leqslant 35$. (For each chosen value of f we draw the *attractor(s)* by plotting the total population size, $x(t) + y(t)$, for $10\,000 \leqslant t \leqslant 10\,500$, starting with 50 random initial conditions.) The dotted lines indicate unstable periodic points, which must be computed separately using a root finding algorithm.

We now discuss the salient features of the bifurcation diagram. We remark that since this is mainly a numerical study, all bifurcation values are approximate.

At $f = 14.9$, there is a period-3 saddle-node bifurcation that produces an attracting period-3 orbit and its associated period-3 (unstable) saddle orbit. For $14.9 < f < 18.13$, the attracting fixed point coexists with the new period-3 attracting orbit. At $f = 18.13$, the stable fixed point undergoes a supercritical Hopf bifurcation, which creates a smooth invariant attracting closed curve.

The period-3 saddle-node bifurcation and Hopf bifurcation are followed for large parameter values by various local and global bifurcations that we analyse later.
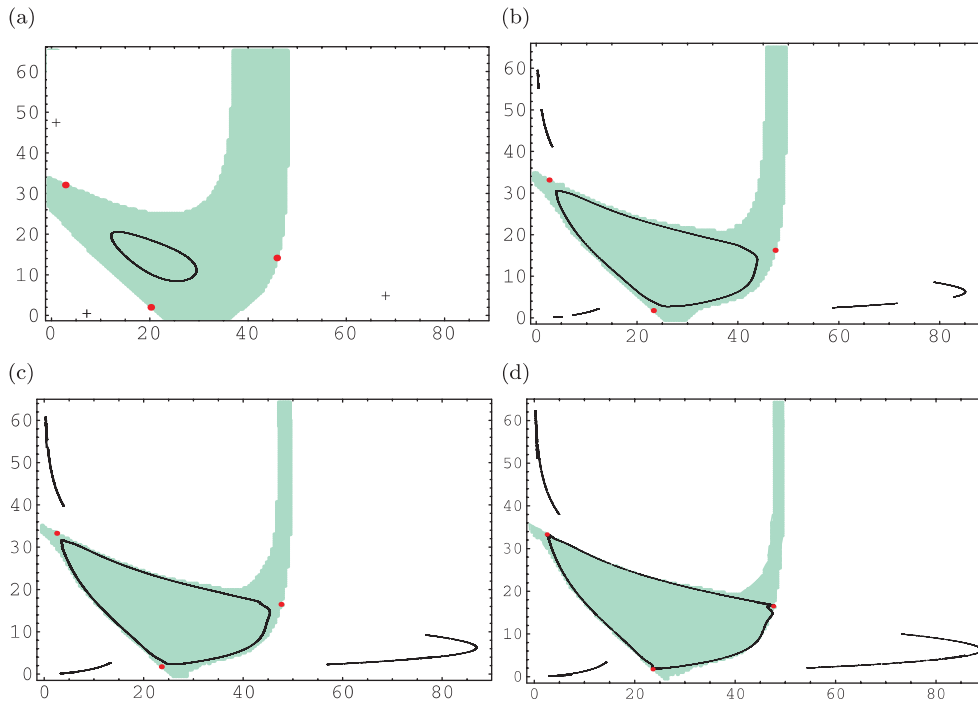
Figure 2. Multiple attractors and their basins: the basin of the attracting 'loop' is the coloured region, while the basin of the other attractor is the white region; the basin boundaries are given by the stable manifolds of the period-3 saddle orbit (marked with '●'). (a) $f = 19$: a period-3 attracting cycle coexists with an invariant closed curve. (b) $f = 23.1$: a six-piece Hénon-like attractor coexists with an invariant closed curve. (c) $f = 23.6$: a three-piece Hénon-like attractor coexists with an invariant closed curve. (d) $f = 24.19$: a three-piece Hénon-like attractor coexists with a new strange attractor (formerly a closed invariant curve), see figure 11 for enlargement showing fractal structure.

First, we briefly illustrate the complexity of the bifurcation scenarios with several examples for $14.9 < f < 24.195$ (figure 2), where there exist two different transitive attractors, each with a large basin of attraction.

At $f = 19$, a period-3 attracting orbit (marked with '+') coexists with a smooth invariant attracting closed curve (figure 2(a)). The boundaries of the basins of attraction are given by the stable manifolds of the period-3 saddle orbit (the period-3 saddle cycle is marked with '●').

At $f = 23.1$, a six-piece Hénon-like strange attractor coexists with an attracting invariant curve (figure 2(b)). At $f = 23.6$, a three-piece Hénon-like attractor coexists with an invariant closed curve (figure 2(c)). This invariant closed curve bifurcates into a strange attractor, and the boundaries of the basins of attraction are still given by the stable manifolds of the period-3 saddle orbit. At $f = 24.19$, a three-piece Hénon-like attractor coexists with the new strange attractor (figure 2(d)). See figure 11 for an enlargement showing the fractal structure.

The next subsections contain a more thorough discussion of these bifurcation scenarios.

5.1. Evolution of the period-3 attracting orbit

The period-3 attracting orbit undergoes a period doubling cascade at $f = 19.9, 22.2, 22.7, \ldots$, which produces attracting periodic orbits with periods $3 \cdot 2^n$, $1 \leqslant n < \infty$. Immediately after
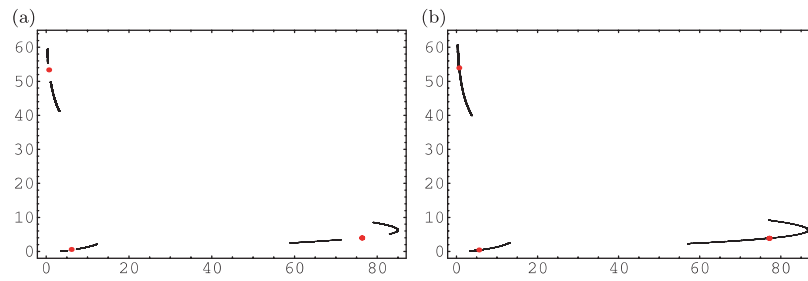
Figure 3. Hénon-like attractors and merging. (*a*) Six-piece Hénon-like attractor ($f = 23.07$). (*b*) Pairwise merging at $f = 23.55$.
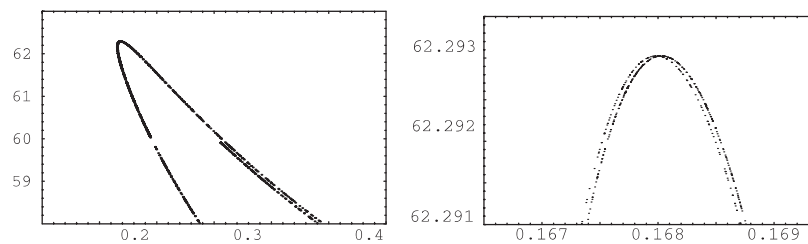

Figure 4. Zoom-in for a Hénon-like component at $f = 23.55$.

that, strange attractors exist. For $23.07 < f < 23.55$, the strange attractor consists of a six-piece Hénon-like attractor (see figure 3(*a*)). The three pairs of branches of the attractor undergo a merging crisis at $f = 23.55$, which results in a three-piece Hénon-like attractor (see figures 3(*b*) and 4). The merging is mediated by a period-3 saddle orbit. The three-piece Hénon-like attractor coincides with the closure of the unstable manifold of the period-3 saddle point.

At $f = 31$, an explosion of the size of the strange attractor occurs due to an interior crisis mediated by another period-3 saddle orbit (see figure 5(*d*)). Now, the attractor consists of only one piece. See also [11] for the case $p_1 = 1$.

In the next subsection, we study the evolution of the invariant curve obtained after the Hopf bifurcation as the parameter f increases.

5.2. Bifurcation cascade of invariant closed curve to strange attractor

The attracting curve undergoes a complicated transition to chaos (see also [1] for a panorama of possible behaviour for a two-parameter family of planar diffeomorphisms). This transition involves phase locking, homoclinic and heteroclinic intersections, invariant attracting closed curves bifurcating into strange attractors, transient chaos, loss of smoothness, saddle-node bifurcations and the appearance of strange attractors.

At $f = 23.7$, a period-14 phase locking occurs on the invariant closed curve and persists until $f = 23.93$. Figure 6 shows the *invariant curve in resonance* at $f = 23.85$. By this, we mean the period-14 attracting orbit connected by the unstable manifolds of the period-14 saddle points (homoclinic connections). This closed curve is not an attractor; most nearby points are attracted to the sinks, and its smoothness is determined by the way the unstable manifolds of two successive saddle points join at the periodic sink [1].

The invariant closed curve in resonance is destroyed at $f = 23.9367$ due to a homoclinic tangency: the stable and unstable manifolds of two adjacent period-14 saddle points are tangent,
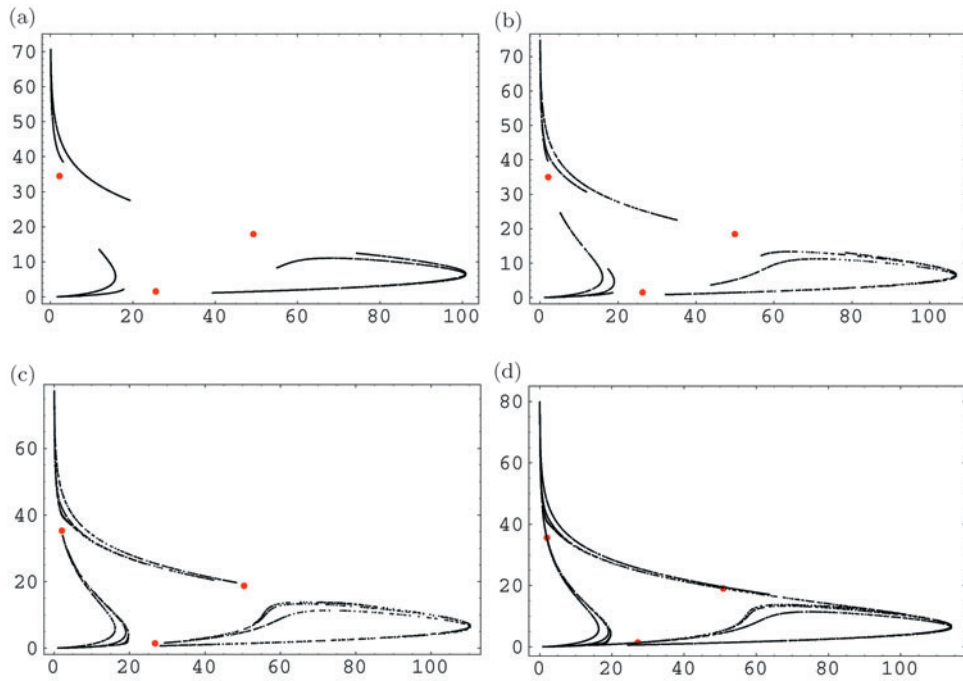
Figure 5. Strange attractors for $f = 27, 29, 30, 31$. At $f = 31$, an interior merging crisis occurs, mediated by the period-3 saddle orbit. (*a*) $f = 27$; (*b*) $f = 29$; (*c*) $f = 30$; (*d*) $f = 31$.
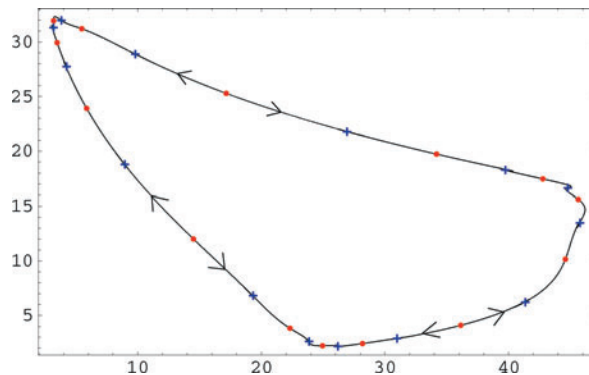

Figure 6. Period-14 phase locked invariant curve at $f = 23.85$.

see figure 7(*b*). After the homoclinic tangency, we have transversal homoclinic intersections (figure 7(*c*)), which produce chaotic horseshoes. Although this phenomenon creates chaotic dynamics, the 'visible' attractor is still a period-14 orbit.

Next, we describe the mechanism that leads to the appearance of the strange attractor. At $f = 23.9866$, another saddle-node bifurcation creates a period-31 attracting orbit (and its associated period-31 saddle orbit), which coexists until $f = 23.9889$, with the period-14 attracting orbit. Figure 8 shows a part of the bifurcation diagram for this parameter interval, with two of the period-14 saddle-node pairs and three saddle-node pairs of period-31.
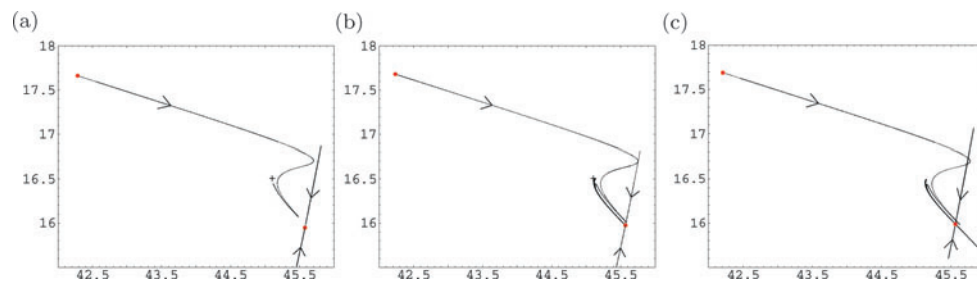
Figure 7. Homoclinic intersections. (*a*) $f = 23.93$: before homoclinic tangency. (*b*) $f = 23.9367$: homoclinic tangency. (*c*) $f = 23.95$: transversal homoclinic intersections.
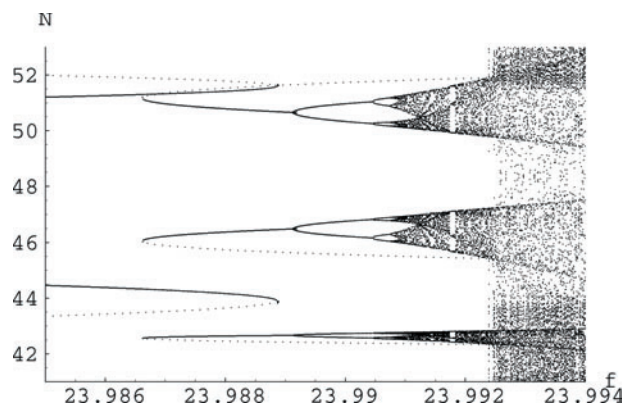

Figure 8. Part of the bifurcation diagram for $23.984 < f < 23.994$.

Remark. The rotation number of the period-14 orbit is $\frac{5}{14}$, while the rotation number of the period-31 orbit is $\frac{11}{31}$. Note that $\frac{5}{14}$ and $\frac{11}{31}$ are consecutive numbers in the Farey sequence (see [1] for details) since $5 \cdot 31 - 14 \cdot 11 = 1$. We thank Henk Bruin for this observation.

At $f = 23.9889$, the period-14 attracting orbit is annihilated after colliding with its associated period-14 saddle orbit, and at $f = 23.989$, the period-31 orbit initiates a period doubling cascade. This will lead to a 31-piece Hénon-like transitive strange attractor (see figure 9 for $f = 23.992$).

For $f = 23.99237$, an interior crisis occurs (the 31-piece strange attractor collides with the period-31 saddle orbit created at $f = 23.9866$). See figure 10. As a consequence, the 31-piece strange attractor suddenly increases its size (figure 11) since it will now contain all branches of the unstable manifolds of the period-31 saddle. Unfortunately we are so far unable to find a homoclinic tangency that produces this interior crisis.

Although the former curve in resonance 'appears reconstructed', the collision results in a strange attractor (figure 11). Thus the bifurcation route from the invariant attracting closed curve to strange attractor is subtle, involving the creation and annihilation of period-14 and -31 orbits along the way. It does not occur instantaneously.

This strange attractor will be destroyed by a boundary crisis at $f = 24.195$ (figure 12). There is a collision between this attractor and the boundary of its basin of attraction given by the stable manifold of the period-3 saddle orbit obtained at $f = 14.9$. At this boundary crisis, the attractor coincides with the closure of a branch of the unstable manifold of the
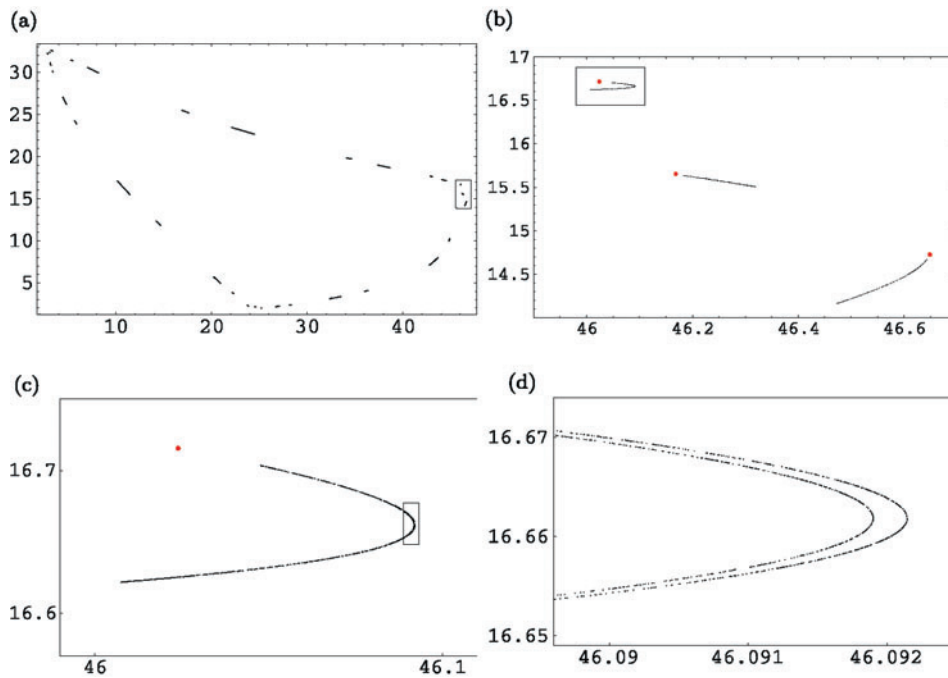
Figure 9. Thirty-one-piece strange attractor and consecutive enlargements ($f = 23.992$). (*a*) Thirty-one-piece strange attractor. (*b*) Blow-up of (*a*). (*c*) Blow-up of (*b*). (*d*) Blow-up of (*c*).
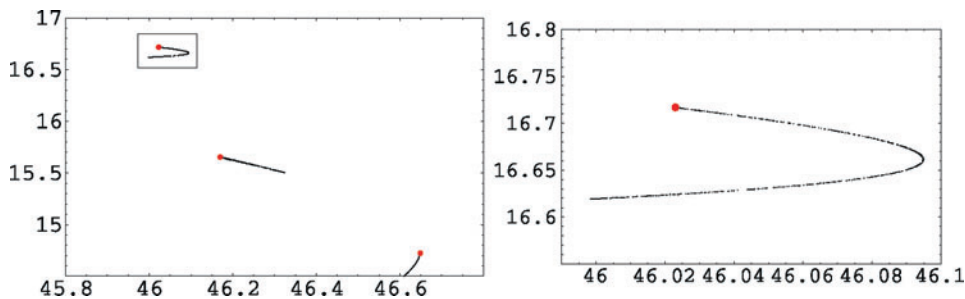

Figure 10. Interior crisis at $f = 23.99237$: the 31-piece strange attractor collides with a period-31 saddle orbit.

period-3 saddle orbit. Therefore, the boundary crisis is mediated by a homoclinic tangency (figure 13(*b*)). The Newhouse conditions are easily checked in this case and one would expect to find infinitely many sinks for nearby parameter values [22, 23]. We have not been able to find these, probably because they have tiny basins.

After the homoclinic tangency, the strange attractor disappears, but we have transient chaos (existence of chaotic horseshoes due to transversal homoclinic intersections). Figure 14(*b*) was obtained by plotting the trajectory of an orbit with an initial condition taken from the basin of the old attractor. We noticed that the orbit spends a considerable amount of time around the old attractor (for $1 \leqslant t \leqslant 2200$) before moving towards the new attractor. This phenomenon has direct implications for a population model since, for a significant time period, the behaviour is dictated by transient dynamics.
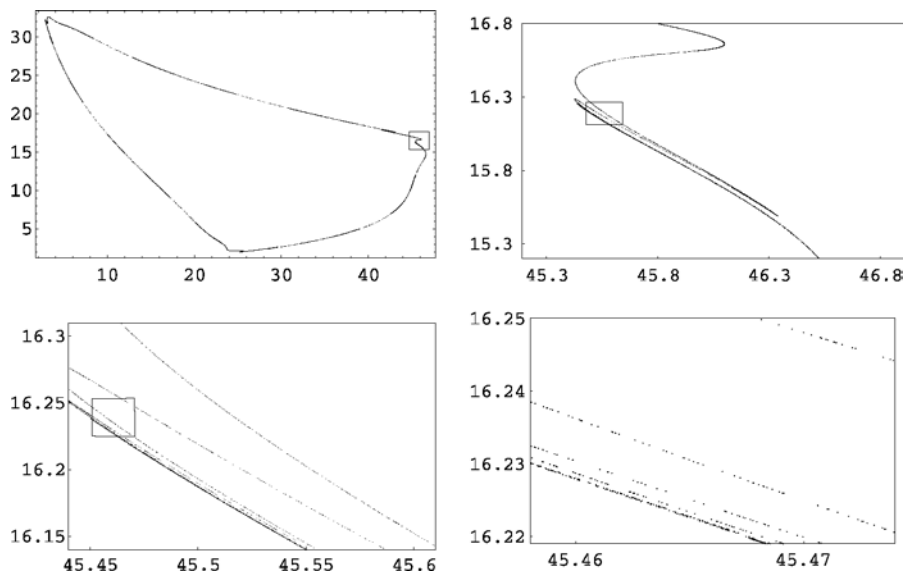
Figure 11. Strange attractor at $f = 23.993$, and a sequence of enlargements showing the fine structure at the tip of the attractor.
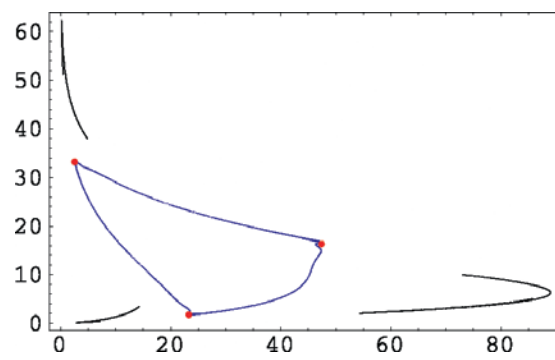

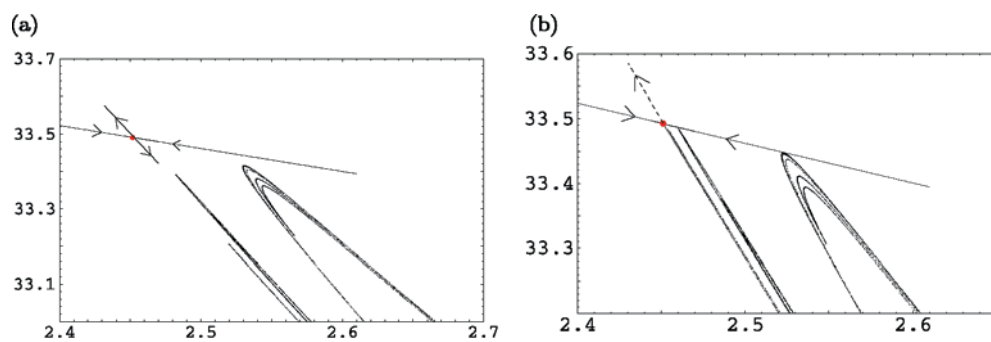**Figure 12.** Boundary crisis at $f = 24.195$.

Figure 13. Homoclinic tangency and boundary crisis. (*a*) Before boundary crisis ($f = 24.19$). (*b*) Boundary crisis at $f = 24.195$.
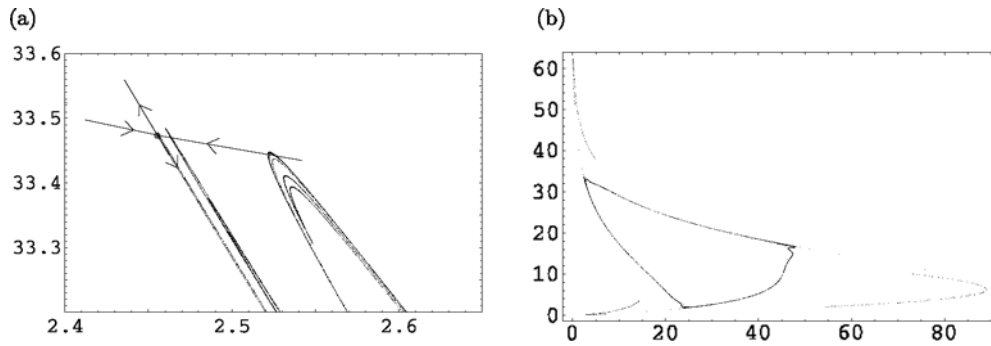
(a)

(b)

Figure 14. Transverse homoclinic intersections (*a*) and transient chaos (*b*) at $f = 24.2$.
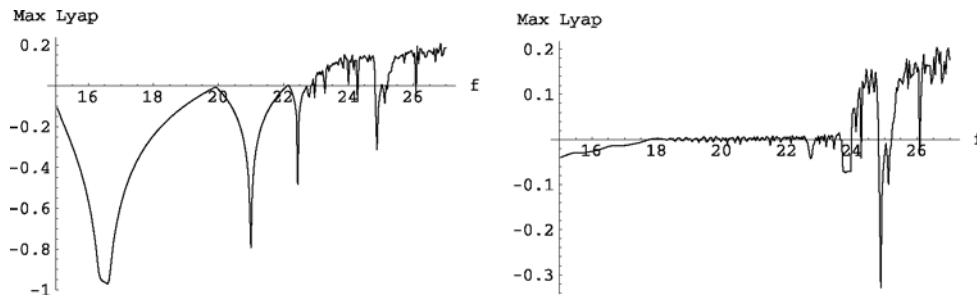

Figure 15. Plots of dominant Lyapunov exponent of orbits with different initial conditions.

We cannot find any new phenomena appearing in the bifurcation diagram for $f \geqslant 31$. The phase portrait contains a Hénon-like strange attractor with occasional periodic windows.

We finish this section with two plots representing the dominant Lyapunov exponent for $15 \leqslant f \leqslant 27$ (figure 15) of forward orbits starting from two different initial conditions corresponding to the two coexisting attractors discussed above. We used the algorithm described in [30] to compute the Lyapunov exponents.

6. Three-generation model

In this section, we study the three-generation model with equal fertility rates $f = f_1 = f_2 = f_3$ and fixed survival probabilities $p_1 = 0.8$, $p_2 = 0.6$. The time-advance mapping is given by

$$T(x, y, z) = (f \cdot (x + y + z)e^{-0.1(x+y+z)}, 0.8x, 0.6y).$$

We observe many of the same global bifurcations and complicated dynamics as we did for the two-generation model. The main differences involve an interesting new bifurcation scenario of attracting closed curve into strange attractor (see subsection 6.1) and the 'filling-in' phenomenon resulting in a sudden increase of the fractal dimension for the strange attractor.

The bifurcation diagrams for $20 \leqslant f \leqslant 45$ and $45 \leqslant f \leqslant 75$ are shown in figure 16. In what follows, we list the important dynamical properties that appear in the parameter range $0 < f \leqslant 75$.

(i) The trivial fixed point $(0, 0, 0)$ is globally asymptotically stable for $0 < f < 1/(1 + p_1 + p_1 p_2) = 0.438$. For $f > 0.438$ there exists a nonzero fixed point that is asymptotically stable for small enough f.
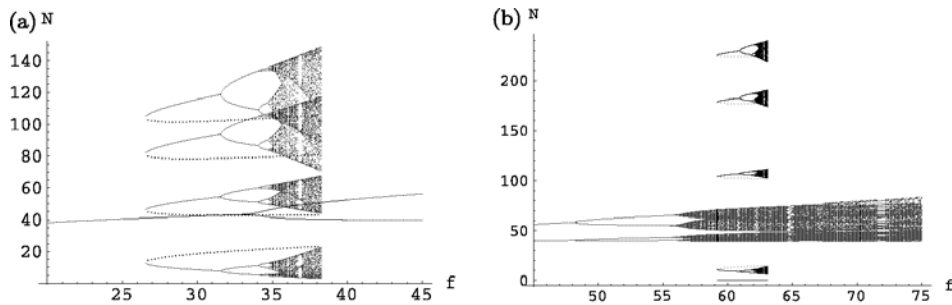
Figure 16. Bifurcation diagrams for $p_1 = 0.8$, $p_2 = 0.6$. (a) $20 \leqslant f \leqslant 45$; ($b$) $45 \leqslant f \leqslant 75$.
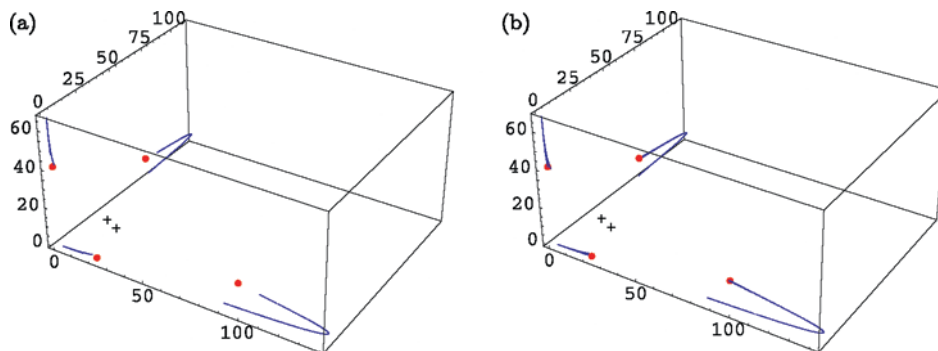

Figure 17. Coexistence of two attractors (a) and boundary crisis (b). (a) A four-piece Hénon-like attractor and a period-2 cycle coexist at $f = 37.5$. (b) Boundary crisis at $f = 38.3$: the four-piece Hénon-like attractor is destroyed.

(ii) A saddle-node bifurcation occurs at $f = 26.7$, creating a period-4 attracting orbit that coexists with the stable fixed point. The period-4 orbit undergoes a period doubling cascade ($f = 31.6, 34.1, 34.7, 34.75, \ldots$). Strange attractors appear after the period doubling limit.

(iii) Multiple attractors coexist for $26.7 \leqslant f \leqslant 38.3$. Figure 17($a$) shows a four-piece Hénon-like attractor and a period-2 attracting cycle (marked by '+'). The period-4 saddle orbit is marked by '•'.

(iv) The fixed point undergoes a period doubling bifurcation at $f = 34$.

(v) At $f = 38.3$, the strange attractor is destroyed due to a collision with the period-4 saddle. This is a boundary crisis and results in a large discontinuous decrease in population (figure 17(b)). After the boundary crisis, the only attractor left is the period-2 orbit.

(vi) The period-2 sink bifurcates into a period-4 sink (period doubling bifurcation at $f = 48.5$).

(vii) The period-4 sink undergoes a Hopf bifurcation at $f = 55.5$; four attracting smooth closed curves are born (see figure 18 for $f = 58$).

(viii) A period-5 orbit is born at $f = 59.4$, after a saddle-node bifurcation.

(ix) Multiple transitive attractors coexist for $59.4 \leqslant f \leqslant 63.1$ (see figure 19).

(x) The period-5 sink undergoes a period doubling cascade, which will lead to Hénon-like strange attractors.

(xi) There is a merging crisis of two pairs of attracting closed curves at $f = 59$.

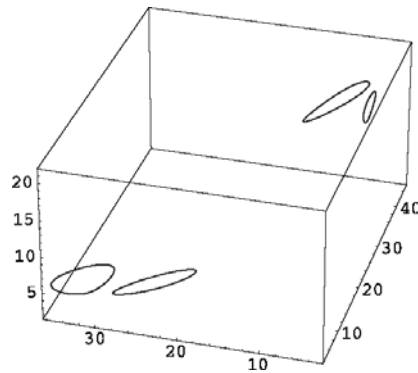(xii) There is a boundary crisis at $f = 63.1$. The Hénon-like strange attractor is destroyed.

Figure 18. $f = 58$: the transitive attractor consists of four smooth closed curves visited in a cyclic manner.
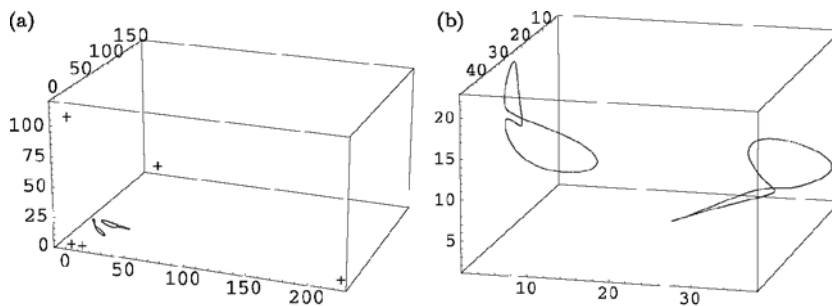

Figure 19. Coexisting attractors at $f = 60$. (*a*) A period-5 orbit coexists with two closed curves. (*b*) Zoom-in of the two closed curves.

(xiii) At $f = 66$ there are two attracting T^2-invariant closed curves[1]. As f increases these two closed curves bifurcate into a pair of strange attractors. As f further increases, the two strange attractors *fill-in* and merge. Figure 20 shows the corresponding sequence of bifurcations. In the following subsection we explain the bifurcation route leading from two smooth invariant curves to a strange attractor.

6.1. Bifurcation cascade of attracting closed curves to strange attractor

At $f = 66.5$ a period-52 saddle-node bifurcation occurs. Figure 21(*a*) shows the coexistence of two attracting T^2-invariant closed curves and a period-52 attracting orbit. At $f = 66.935$ a new period-48 saddle-node bifurcation occurs. For $66.935 \leqslant f \leqslant 67.11$ at least three transitive attractors coexist: two T^2-invariant closed curves, a period-52 orbit, and a period-48 orbit. At $f = 67.11$ there is a boundary crisis between the closed curves and the period-48 saddle, which leads to the destruction of the closed curves (figure 22).

Between $67.11 < f < 67.7$ the period-48 attracting orbit coexists with the period-52 attracting orbit.

The period-48 cycle exhibits a Hopf bifurcation at $f = 67.97$ (figure 23(*a*)). Figure 24 shows a transitive attractor consisting of 48 T^{48}-invariant closed curves. The 48 invariant
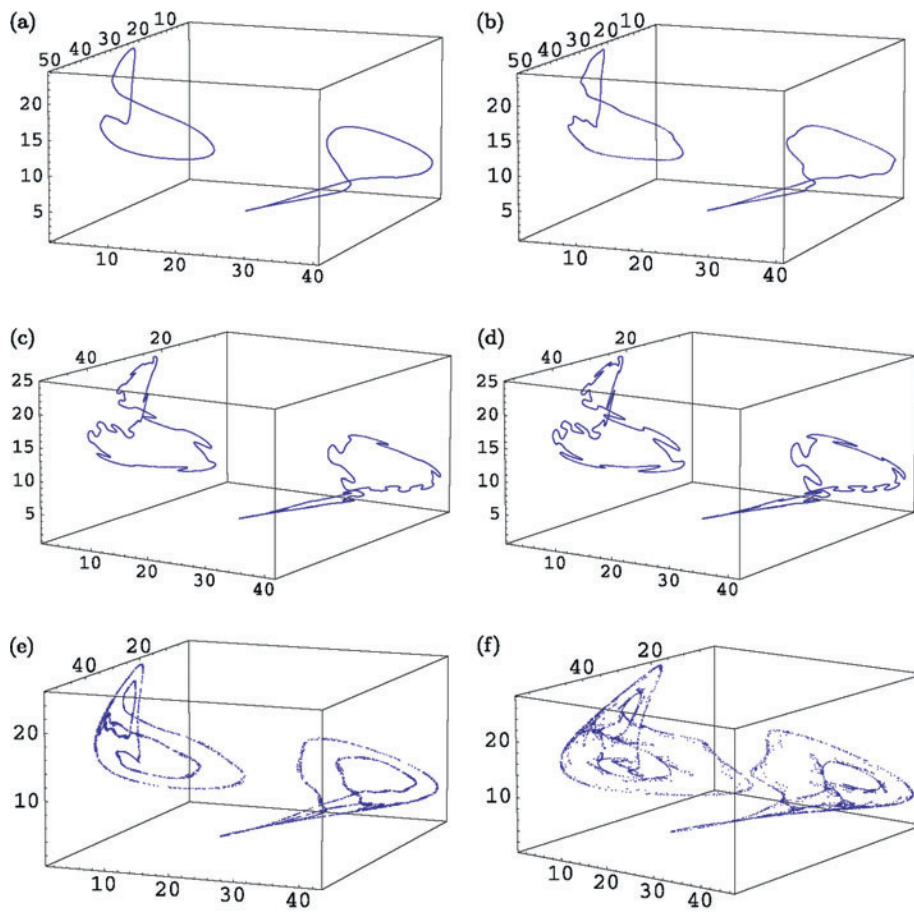
---

[1] Here T^2 denotes the second iterate of the mapping T.

Figure 20. Bifurcation of closed curves to strange attractor. (*a*) $f = 66$; (*b*) $f = 66.7$; (*c*) $f = 67$; (*d*) $f = 67.084$; (*e*) $f = 68.2$; (*f*) $f = 74$.
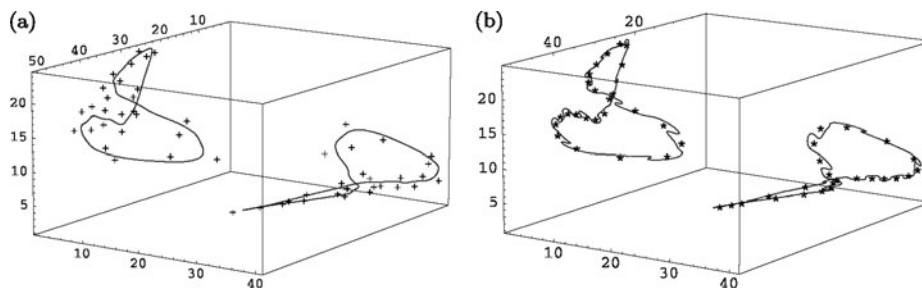

Figure 21. Periodic orbits coexist with T^2-invariant curves. (*a*) A period-52 attracting orbit appears off the invariant curves at $f = 66.5$, after a saddle-node bifurcation. (*b*) A period-48 attracting orbit appears off the invariant curves at $f = 66.935$, after a saddle-node bifurcation.

loops are destroyed in a boundary crisis at $f = 67.99$ (they collide with a period-48 saddle orbit). The period-52 stable orbit starts a period doubling cascade at $f = 67.7$ (figure 23(*b*)). After the period doubling limit, a 2×52-piece Hénon-like transitive strange attractor is born (figure 25(*a*)).
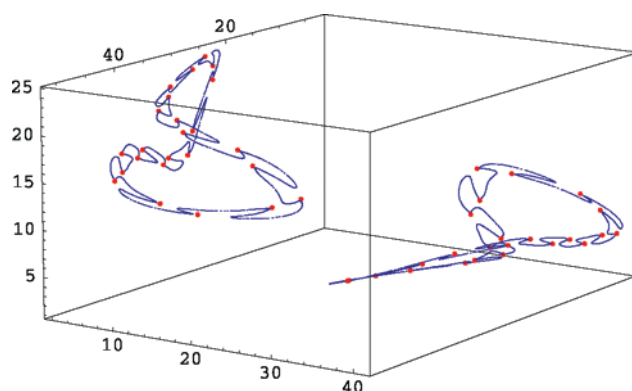
Figure 22. Boundary crisis at $f = 67.11$: the two closed curves collide with a period-48 saddle orbit.
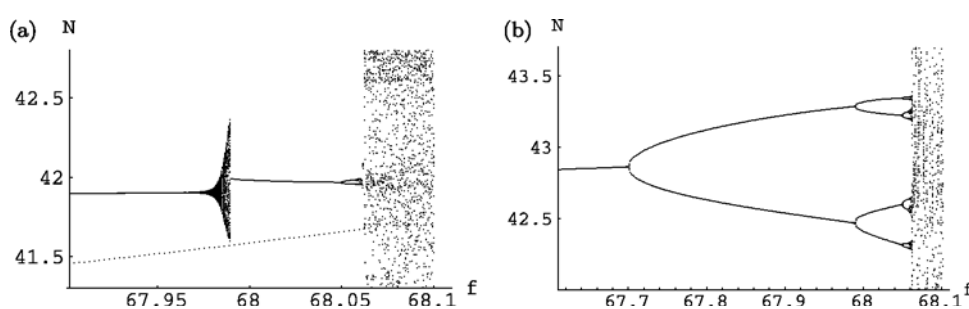

Figure 23. Evolution of period-48 and period-52 attracting orbits. (*a*) Bifurcation diagram for T^{48} shows a Hopf bifurcation at $f = 67.97$: the dotted line represents a period-48 saddle. (*b*) Bifurcation diagram for T^{52}: a period doubling cascade starts at $f = 67.7$.
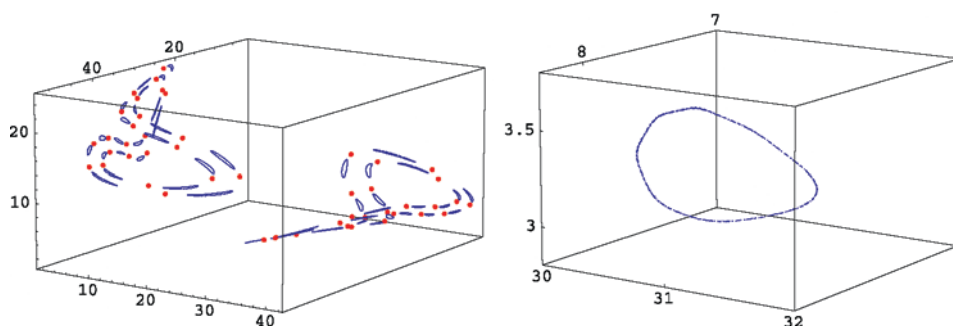

Figure 24. Transitive attractor consisting of 48 closed curves at $f = 67.98$ (left) and enlargement of one closed curve (right).

We are currently investigating the bifurcation route from the Hénon-like attractors to the attractor shown in figure 25(*b*). In the two-dimensional model we show that this explosion in the size of the strange attractor is due to an interior crisis. This case is more subtle because the fractal dimension of the strange attractor seems to jump (and visually becomes 'thicker'), which does not occur in the two-dimensional model. This phenomenon might be a manifestation of the noninvertibility of the mapping T; it might result from the interaction of the degenerate locus
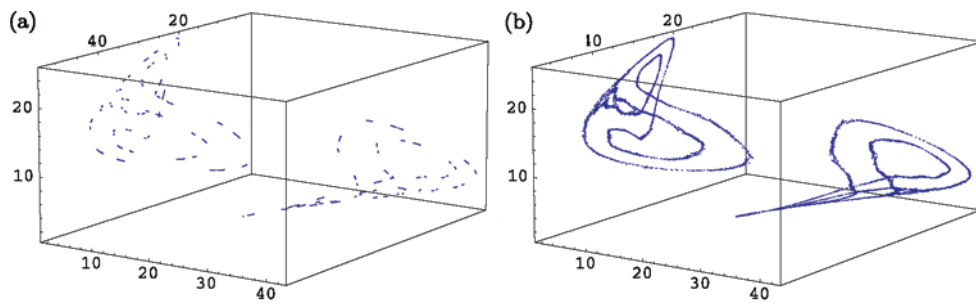
Figure 25. Strange attractors. (*a*) 2×52-piece Hénon-like transitive attractor at $f = 68.06$. (*b*) Strange attractor at $f = 68.08$.
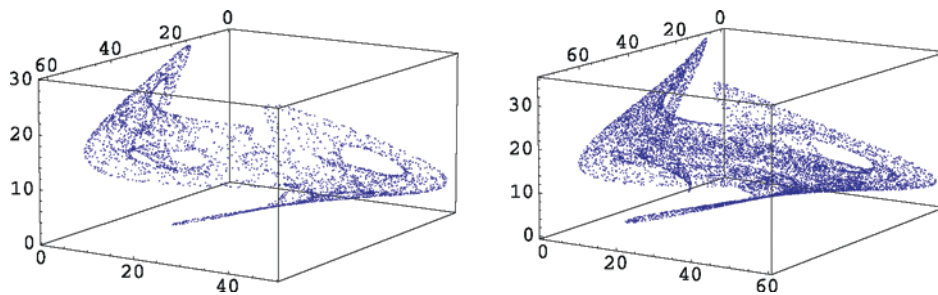

Figure 26. Strange 'fat' attractors at $f = 77$ (left) and $f = 100$ (right).

with the basin boundary (see [20] for possible scenarios for two-dimensional noninvertible maps). Figure 26 shows the existence of 'fat' strange attractors obtained for larger values of the parameter f.

We observe some key differences between the three-dimensional model (with $f = f_1 = f_2 = f_3$) and the two-dimensional model (with $f = f_1 = f_2$):

- In the two-dimensional system the Hénon-like attractor obtained after the period doubling cascade is the one that will persist for large values of the parameter f, and the 'invariant loop' strange attractor is destroyed in a boundary crisis. In the three-dimensional case, the Hénon-like attractors are destroyed in a boundary crisis, and for large values of the parameter f, the invariant loop attractor persists.
- The invariant curve in the two-dimensional model is born after a Hopf bifurcation of the positive equilibrium point, while in the three-dimensional situation, the positive fixed point first undergoes two period doubling bifurcations and then the stable four cycle undergoes a Hopf bifurcation creating four attracting closed curves.

7. Concluding remarks

We have shown that the two- and three-generation Leslie models with exponentially damped fertility exhibit a huge variety of complicated dynamical behaviour, including many forms of chaotic behaviour. It seems essential to understand the implications for the population of the chaotic behaviour. Already in [19] May has commented about the 'disturbing practical

applications' of chaos in population models, and there has been a great deal of discussion about this in the population biology literature.

The models in this paper exhibit crises, which can result in sudden large population swings and which by definition require the presence of strange attractors. These models also exhibit bifurcations of stable attracting cycles into strange attractors, a seemingly new path to chaos in population models. The various *periodicities* of the attractors in these models, e.g. the three-piece strange attractor in figure 2(c) in which points in the basin cycle lie chaotically around the three pieces, produce an intriguing combination of cyclic yet chaotic behaviour for the population.

Although most population biologists seem to strongly believe that initial conditions are irrelevant to the long term behavior of populations, we discovered robust parameter ranges with coexisting strange attractors with large basins, for which the population biologists' notion of ergodicity fails in an essential way. We are currently studying the existence and statistical properties of SRB, or natural measures on these attractors, which should also help make the notion of ergodicity more rigorous.

Even though it is usually impossible to make long term predictions about chaotic systems, Grebogi *et al* [25] have pioneered the study of 'controlling chaos', and some of their techniques may be useful for controlling populations exhibiting chaotic behaviour.

One colleague commented that the complicated dynamics we observe is not surprising since May [19] has shown that the one-dimensional logistic family already exhibits complicated dynamical behaviour, and furthermore, one would expect a nonlinear dynamical system with several parameters to exhibit a large variety of complicated dynamical behaviour. Our reply is that we have studied the dynamics of several multi-parameter nonlinear population models in the literature, including the famous models in [8] and [18], and found that they all exhibit a much smaller variety of complicated dynamical behaviour. Also, although there is a vast literature on modelling physical and biological phenomena, the authors are unaware of *any* low dimensional dynamical system, from any field, that exhibits a richer variety of complicated dynamical behaviour. Finally, we stress that the model we consider is a natural extension of the ubiquitous Leslie population model and was suggested by several prominent population biologists.

This investigation is the first step of our programme to study systematically the global dynamics and bifurcations for nonlinear Leslie models where the fertility rates and survival probabilities have various natural functional forms. Our ultimate goal is to create a 'population modelling toolbox' that could be used by a wide range of population modellers to predict animal populations more accurately.

Acknowledgments

Appendix

A.1. Stable and unstable manifolds

Let us recall that if $F : U \subset \mathbb{R}^d \to \mathbb{R}^d$ is a C^1 mapping and if p is a hyperbolic fixed point with linear splitting $T_p U = E^{\mathrm{s}} \oplus E^{\mathrm{u}}$, then there exists a local stable manifold $W^{\mathrm{s}}_{\mathrm{loc}}(p)$

and a local unstable manifold $W_{\text{loc}}^{\text{u}}(p)$ tangent at p to E^{s} and E^{u} and satisfying the following properties:

(1) $W_{\text{loc}}^{\text{s}}(p)$ and $W_{\text{loc}}^{\text{u}}(p)$ are F-invariant, i.e.

$$F(W_{\text{loc}}^{\text{s}}(p)) \subset W_{\text{loc}}^{\text{s}}(p) \qquad \text{and} \qquad F(W_{\text{loc}}^{\text{u}}(p)) \supset W_{\text{loc}}^{\text{u}}(p).$$

(2) There are constants $C > 0$ and $0 < \lambda < 1$ such that for any $n \in \mathbb{N}$ one has the relations that $d(F^n x, F^n y) \leqslant C\lambda^n d(x, y)$ for $x, y \in W_{\text{loc}}^{\text{s}}(p)$ and $d(F^n x, F^n y) \geqslant C\lambda^{-n} d(x, y)$ if $F^k x, F^k y \in W_{\text{loc}}^{\text{u}}(p)$ for $k = 1, \ldots, n$.

(3) There exists $\delta > 0$ such that

$$W_{\text{loc}}^{\text{s}}(p) = \{x \in U : d(F^n x, p) \leqslant \delta \text{ for all } n \in \mathbb{N}\}$$

and

$$W_{\text{loc}}^{\text{u}}(p) = \{x \in U : \text{ there exists } x_n \in F^{-n}(x) \text{ such that } d(F^k x_n, p) \leqslant \delta$$
$$\text{for all } n \in \mathbb{N} \text{ and } k = 1, \ldots, n\}.$$

The *global stable and unstable manifolds* (see, e.g., [20, 26]) are defined by

$$W^{\text{s}}(p) = \bigcup_{n \in \mathbb{N}} F^{-n}(W_{\text{loc}}^{\text{s}}(p)) = \{x \in U : d(F^n(x), p) \to 0\}$$

$$W^{\text{u}}(p) = \bigcup_{n \in \mathbb{N}} F^n(W_{\text{loc}}^{\text{u}}(p)) = \{x \in U : \exists x_n \in F^{-n}(x) \text{ such that } d(x_n, p) \to 0\}.$$

A.2. Lyapunov exponents

The dominant Lyapunov exponent associated with a forward orbit $\{T^n(x)\}_{n \geqslant 0}$ is defined by

$$\lambda(x) = \limsup_{n \to \infty} \frac{1}{n} \log \|DT^n(x)\|.$$

A positive dominant Lyapunov exponent indicates an infinitesimal chaotic orbit. For a comprehensive presentation of dynamical systems with nonzero Lyapunov exponents, see [2, 27] or the supplement of [15].

A.3. Strange attractors

There exist several definitions, in the literature, for strange (chaotic) attractors. In this paper, by *strange attractor* we mean a compact invariant set Λ having a dense orbit with positive Lyapunov exponent (sensitive dependence on initial conditions) and whose basin of attraction has a nonempty interior (or even more restrictive, Λ is included in the interior of its basin).

Following [26], a strange attractor Λ is *Hénon-like* if besides the properties mentioned above, Λ coincides with the closure of the unstable manifold of a hyperbolic (saddle) periodic point and Λ is not a hyperbolic set.

A.4. Crises

In a series of highly cited papers, Grebogi, Ott and Yorke have undertaken a systematic study of crises. Following [10], a crisis is defined to be a collision between a (strange) attractor and a coexisting unstable fixed point or periodic orbit. Crises appear to be the cause of most sudden changes in chaotic dynamics. There are three types of crises:

- *Boundary crisis*: leads to sudden destruction of the chaotic attractor and its basin. The unstable orbit that collides with the strange attractor is on the boundary of the basin.

- *Interior crisis*: leads to sudden increases in the size of the attractor. The unstable orbit that collides with the strange attractor is situated within the basin of attraction.
- *Merging crisis*: two or more chaotic attractors merge to form one chaotic attractor.

In almost all known two-dimensional examples, an interior or boundary crisis occurs at a parameter value where there is a homoclinic (heteroclinic) tangency of the stable and unstable manifolds.

References

[1] Aronson D G, Chory M A, Hall G R and McGehee R P 1982 Bifurcations from an invariant circle for two-parameters families of maps of the plane: a computer assisted study *Commun. Math. Phys.* **83** 303–54
[2] Barreira L and Pesin Ya 2002 *Lyapunov Exponents and Smooth Ergodic Theory* (*University Lecture Series* vol 23) (Providence, RI: American Mathematical Society)
[3] Benedicks M and Carleson L 1991 The dynamics of the Hénon map *Ann. Math.* **133** 73–169
[4] Caswell H 2001 *Matrix Population Models* 2nd edn (Sunderland, MA: Sinauer)
[5] Conser R J, Hill K T, Crone P R, Lo N C H and Bergen D 2002 *Stock assessment of Pacific sardine with management recommendations for 2002*, Pacific Fishery Management Council, Portland, Oregon
[6] Curry J H and Yorke J A 1978 A transition from Hopf bifurcation to chaos: computer experiments with maps on R^2 *Proc. Conf. North Dakota State University (Fargo, ND, 1977)* (*Lecture Notes in Mathematics* vol 668) (Berlin: Springer) pp 48–66
[7] Cushing J M 1998 *An Introduction to Structured Population Dynamics* (*CBMS-NSF Regional Conf. Series in Appl. Math.* vol 71) (Philadelphia, PA: SIAM)
[8] Cushing J M, Dennis B, Desharnais R A, Henson S M and Costantino R F 2002 *Chaos in Ecology: Experimental Nonlinear Dynamics* (New York: Academic)
[9] Frouzakis C E, Kevrekidis I G and Peckham B B 2003 A route to computational chaos revisited: noninvertibility and the breakup of an invariant circle *Physica* D **177** 101–21
[10] Grebogi C, Ott E and Yorke J 1983 Crisis, sudden changes in chaotic attractors and transient chaos *Physica* D 181–200
[11] Guckenheimer J, Osher G and Ipaktchi A 1977 The dynamics of density dependent models *J. Math. Biol.* **4** 101–47
[12] Hale J K 1985 *Asymptotic Behavior of Dissipative Systems* (*Math. Surveys Monogr.* vol 25) (Providence, RI: American Mathematical Society)
[13] Hénon M 1976 A two-dimensional mapping with a strange attractor *Commun. Math. Phys.* **50** 69–77
[14] Kan I, Kocak H and Yorke J 1992 Antimonotonicity: concurrent creation and annihilation of periodic orbits *Ann. Math.* **136** 219–52
[15] Katok A and Hasselblatt B 1995 *Introduction to the Modern Theory of Dynamical Systems* (Cambridge: Cambridge University Press)
[16] Leslie P 1945 On the use of matrices in population mathematics *Biometrika* **33** 183–212
[17] Leslie P 1948 Some further notes on the use of matrices in population mathematics *Biometrika* **35** 213–45
[18] Levin S A and Goodyear C P 1980 Analysis of an age-structured fishery model *J. Math. Biol.* **9** 245–74
[19] May R 1976 Simple mathematical models with very complicated dynamics *Nature* **261** 459–67
[20] Mira C, Gardini L, Barugola A and Cathala J-C 1996 *Chaotic Dynamics in Two-dimensional Noninvertible Maps* (Singapore: World Scientific)
[21] Misiurewicz M and Szewc B 1980 Existence of a homoclinic point for the Hénon map *Commun. Math. Phys.* **75** 285–91
[22] Newhouse S 1974 Diffeomorphisms with infinitely many sinks *Topology* **13** 9–18
[23] Robinson C 1983 Bifurcation to infinitely many sinks *Commun. Math. Phys.* **90** 433–59
[24] Ott E 1993 *Chaos in Dynamical Systems* (Cambridge: Cambridge University Press)
[25] Ott E, Sauer T and Yorke J (ed) 1994 *Coping with Chaos* (*Wiley Series on Nonlinear Science*) (New York: Wiley)
[26] Palis J and Takens F 1993 *Hyperbolicity and Sensitive Chaotic Dynamics at Homoclinic Bifurcations* (Cambridge: Cambridge University Press)
[27] Pollicott M 1993 *Lectures on Ergodic Theory and Pesin Theory on Compact Manifolds* (Cambridge: Cambridge University Press)

[28] Pykh Y and Efremova S 2000 Equilibrium, stability and chaotic behavior in Leslie matrix models with different density-dependent birth and survival rates *Math. Comput. Simul.* **52** 87–112

[29] Robinson C 1983 Bifurcation to infinitely many sinks *Commun. Math. Phys.* **90** 433–59

[30] Sandri M 1996 Numerical calculations of Lyapunov exponents *Mathematica J.* 78–84

[31] Silva J A and Hallam T G 1992 Compensation and stability in nonlinear matrix models *Math. Biosci.* **110** 67–101

[32] Silva J A and Hallam T G 1993 Effects of delay, truncation and density dependence in reproduction schedules on stability of nonlinear Leslie matrix models *J. Math. Biol.* **31** 367–95

[33] Simo C 1979 On the Hénon–Pomeau attractor *J. Stat. Phys.* **21** 465–94

[34] Tuljapurkar S and Caswell H 1997 *Structured Population Models in Marine, Terrestrial, and Freshwater Systems* (London: Chapman and Hall)

[35] Wang Q and Young L-S 2002 From invariant curves to strange attractors *Commun. Math. Phys.* **225** 275–304

[36] Wikan A and Mjølhus E 1996 Overcompensatory recruitment and generation delay in discrete age-structured population models *J. Math. Biol.* **35** 195–239

[37] 2002 Demography and the West—Half a billion Americans? *The Economist* 22 August